FULL PAPER

Synthesis and Photophysical Properties of 3,5-Bis(oxopyridinyl)- and 3,5-Bis(pyridinyloxy)-Substituted Boron-Dipyrromethenes

**Tamanna K. Khan,[a] M. Rajeswara Rao,[a] and M. Ravikanth*[a]**

Nucleophilic substitution reactions of 2-, 3- and 4-hydroxy-pyridines with 3,5-dibromo *meso*-aryl and *meso*-furyl boron-dipyrromethenes (BODIPYs) resulted in the formation of the corresponding 3,5-bis(oxopyridinyl)-BODIPYs and 3,5-bis-(pyridinyloxy)-BODIPYs in decent yields. The effect of a pyridone versus an oxypyridine at the 3- and 5-positions on the spectral, electrochemical and photophysical properties were studied as a function of solvent. The 3,5-bis(oxopyridinyl)-BODIPYs exhibit broad, red-shifted absorption and emission bands, decreased quantum yields and lifetimes, displayed large Stokes shifts and easier reductions than did the 3,5-bis(pyridinyloxy)-BODIPYs. The differences in the properties of these two classes of BODIPY dyes are attributed to the extension of π-delocalization associated with the electron-deficient nature of the pyridone groups.

Introduction

2-, 3- and 4-Hydroxypyridines exhibit keto-enol tautomerization between the pyridone and hydroxypyridine form and exhibit interesting chemistry due to the presence of two, different, reactive, nucleophilic centres.[1] The hydroxypyridines would undergo nucleophilic substitution reactions by reacting either through the phenolic oxygen or the pyridine nitrogen, depending on the substrate and reaction condi-

tions. Boron-dipyrromethene (BODIPY) dyes are interesting fluorescent dyes with valuable properties such as high chemical and photostability and relatively high absorption coefficients and fluorescence quantum yields.[2] Furthermore, BODIPY dyes can be optically excited with visible light, and their absorption and emission properties can be fine tuned by introducing appropriate substituents onto the BODIPY framework.[3] The substituents can be introduced onto any position of the BODIPY framework, although the
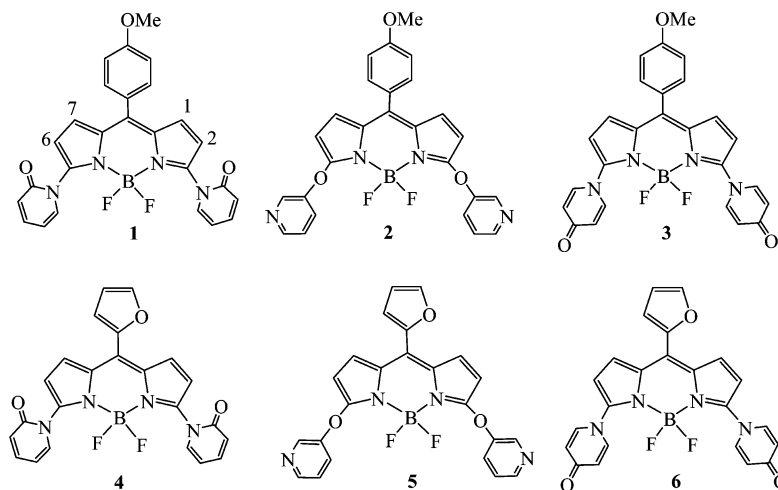
Scheme 1. Structures of **1**–**6**.

[a] Department of Chemistry, Indian Institute of Technology, Powai,
    Mumbai 400076, India
    E-mail: ravikanth@chem.iitb.ac.in
☐ Supporting information for this article is available on the WWW under http://dx.doi.org/10.1002/ejoc.200901460.

electronic properties of BODIPYs are more significantly altered upon introducing substituents directly at the pyrrole C atoms than they are by adding substituents onto the *meso*-aryl group. The *meso*-aryl group and the BODIPY chromophore interact weakly since the two moieties are al-

most perpendicular to each other. Hence, any modifications to the *meso*-aryl group do not alter electronic properties effectively.[4] A more effective way to modulate the properties of the BODIPY chromophore is to introduce aryl groups at the pyrrole carbon atoms (i.e. the 3- and 5-positions). Boens, Dehaen and coworkers[5] recently showed that it is possible to introduce substituents onto a BODIPY chromophore by nucleophilic substitution at the 3- and 5-positions.[5] They used 3,5-dichloro-BODIPY dyes[6] as precursors and prepared a wide range of oxygen-, nitrogen-, sulfur- and carbon-centred nucleophiles substituted at the 3- and 5-positions of BODIPY dyes under very simple reaction conditions.[5] These studies showed that the 3,5-substituents alter the electronic properties of BODIPY dyes significantly, and the properties of the BODIPY dyes depend on the kind of substituents introduced at the 3- and 5-positions.[7] In this paper, we report the synthesis of a new type of 3,5-disubstituted BODIPY, containing pyridone and oxypyridine substituents (**1**–**6**, Scheme 1) and their photophysical properties investigated in various solvents. Although there are several recent reports on 3,5-disubstituted BODIPYs,[7] the oxopyridinyl- and pyridinyloxy-containing BODIPYs are distinctive because they contain hydroxypyridines bonded by nitrogen and oxygen, respectively, at the 3- and 5-positions, which alter their photophysical characteristics significantly, as shown in this paper.

Results and Discussion

To synthesize 3,5-bis(oxopyridinyl)- and 3,5-bis(pyridinyloxy)-substituted BODIPYs **1**–**6**, we needed access to 3,5-dibromo-*meso*-(4-methoxyphenyl)-BODIPY (**9**) and 3,5-dibromo-*meso*-furyl-BODIPY (**12**), which were prepared as shown in Scheme 2. The *meso*-aryl dipyrromethane[8a] **7** and *meso*-furyl dipyrromethane[8b] **10** were treated with 2 equiv. of *N*-bromosuccinimide in THF at –78 °C followed by flash column chromatographic purification on silica to afford 3,5-dibromo-*meso*-aryl dipyrromethane (**8**) and 3,5-dibromo *meso*-furyl dipyrromethane (**11**), respectively, in de-

cent yields (Scheme 2). The 3,5-dibromo dipyrromethanes **8** and **11** were then subjected to a two-step, one-pot reaction by treating them with 1 equiv. of 2,3-dichloro-5,6-dicyano-1,4-benzoquinone (DDQ) followed by $BF_3 \cdot OEt_2$ at room temperature. The progress of the reaction was judged by TLC analysis at regular intervals. The crude reaction mixtures were subjected to silica gel column chromatographic purification and afforded the fluorescent 3,5-dibromo-substituted BODIPYs **9** and **12** in 25 and 42% yield, respectively. Compounds **9** and **12** were confirmed by their molecular-ion peaks in their mass spectra and elemental analysis, which matched the expected composition. In the ^1H NMR spectra, unlike the 3,5-unsubstituted BODIPY, which shows three sets of signals corresponding to three sets of pyrrole protons, **9** and **12** showed only two sets of signals, supporting the substitution of the 3- and 5-positions with bromines. The absorption spectra of **9** and **12** showed a strong absorption band at 520–540 nm, corresponding to the $S_0 \rightarrow S_1$ transition, with a shoulder on the higher-energy side due to the $0 \rightarrow 1$ vibrational transition. In addition, a broad and weak absorption band at <400 nm, corresponding to the $S_0 \rightarrow S_2$ transition, was also present. All these features were in agreement with the reported 3,5-unsubstituted BODIPY dyes.[3] The introduction of bromines at the 3- and 5-positions resulted in an $\approx$ 20 nm red-shift in their absorption bands compared to those of the 3,5-unsubstituted BODIPYs. Furthermore, the **12** showed a 25 nm bathochromic shift in the $S_0 \rightarrow S_1$ absorption band compared to that of **9**, which is attributed to the enhancement of π-delocalization in **12** because the *meso*-furyl group[9] and BODIPY lie in the same plane, unlike in **9**, in which the *p*-methoxyphenyl group is perpendicular to the BODIPY plane.[4]

In the next step, the 3,5-dibromo-BODIPYs **9** and **12** were subjected to nucleophilic substitution reactions by treating them with nucleophiles such as 2-, 3- and 4-hydroxypyridines. The 2- and 4-hydroxypyridines generally exist as the 2-pyridone and 4-pyridone, respectively, whereas the 3-hydroxypyridine exists in the enol form and prefers to react by the phenolic oxygen.[1] Compounds **1**–**3** were prepared by reacting 1 equiv. of **9** with 3 equiv. of 2-hydroxypyridine,
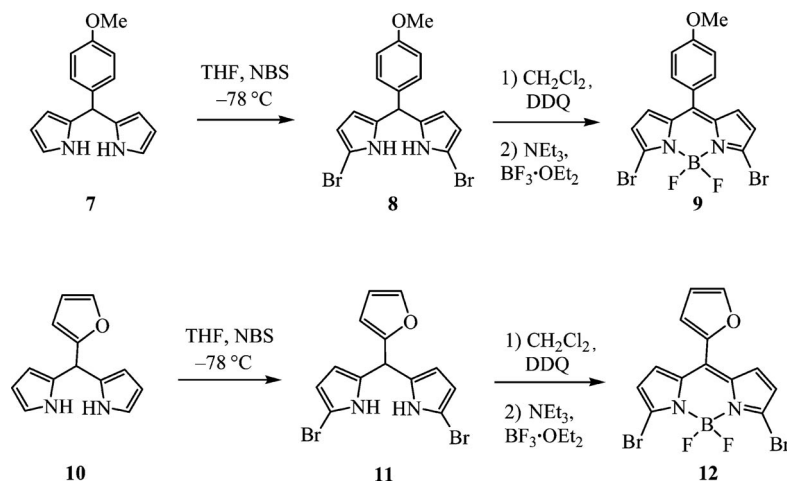
Scheme 2. Synthesis of **9** and **12**.
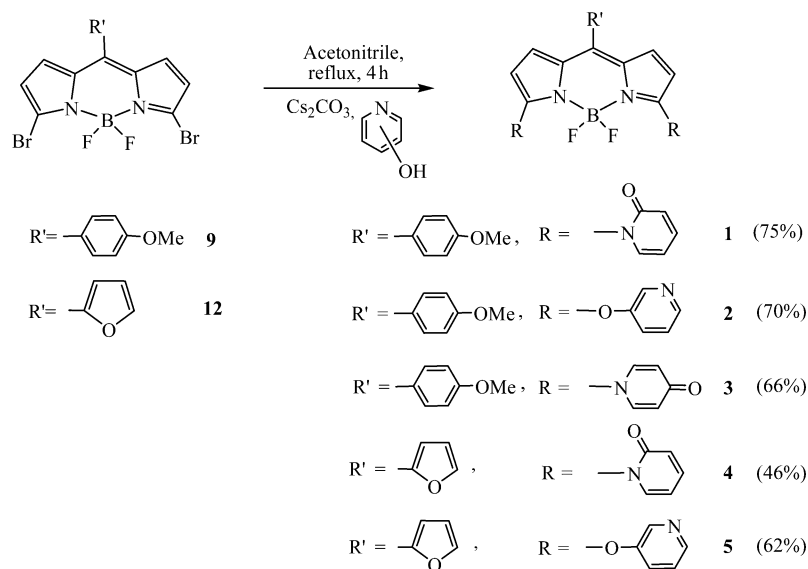
Scheme 3. Synthesis of 3,5-bis(oxopyridinyl)- and 3,5-bis(pyridinyloxy)-substituted BODIPYs **1–5**.

3-hydroxypyridine and 4-hydroxypyridine, respectively, in MeCN in the presence of Cs_2CO_3 at reflux for 1 h. The progress of the reaction was followed by TLC analysis, which indicated the formation of the desired compounds as the sole products. The crude reaction mixtures were subjected to silica gel column chromatography and afforded **1–3** in 66–75% yield (Scheme 3). These reactions worked efficiently with 3 equiv. of nucleophile rather than with 2 equiv., which gave mixtures of products. Similarly, the **4** and **5** were prepared by reacting **12** with 2-hydroxypyridine and 3-hydroxypyridine, respectively, under reaction conditions similar to those used for the synthesis of **1–3**. However, when we treated **12** with 4-hydroxypyridine under similar reaction conditions, although the reaction appeared successful, as judged by absorption spectroscopy and TLC analysis, **6** was very unstable and decomposed on the silica gel column. Several attempts to prepare **6** under various modified reaction conditions failed due to the unstable nature of **6** at room temperature.

Compounds **1–5** were characterized by mass, NMR, absorption and fluorescence spectroscopy and electrochemical and elemental analysis. The molecular-ion peak in the mass spectra and the matching of the elemental analysis with the expected compositions confirmed the identity of **1–5**. ¹H, ¹³C, ¹⁹F and ¹¹B NMR spectroscopy and the colour of the solutions under UV light were used to differentiate BODIPY compounds containing oxypyridines from BODIPY compounds containing pyridones at the 3- and 5-positions. Under UV light, the 3,5-bis(pyridinyloxy)-BODIPYs are more fluorescent than the 3,5-bis(oxopyridinyl)-BODIPYs (Figure S19). A comparison of ¹H and ¹¹B NMR spectra in a selected region for **1–3** is presented in Figure 1, and selected NMR spectroscopic data for **1–5** are presented in Table 1. As is clear from Figure 1 and the data in Table 1, the NMR chemical shifts are very useful in differentiating 3,5-bis(pyridinyloxy)-BODIPYs **2** and **5** from 3,5-bis(oxopyridinyl)-BODIPYs **1**, **3** and **4**. For example, the 1,7-pyrrole protons appeared as a doublet at $\delta = 6.81$ ppm in **2** and experienced a downfield shift to 7.04 in **1** and 7.12 ppm in **3**. Similarly, the 2,6-pyrrole protons, which appeared as a doublet at $\delta = 5.74$ ppm in **2**, experienced an downfield shift in **1** and **3** of about 0.85 ppm (Table 1). The pyridyl protons of **1** and **3** appeared upfield of those of **2**, supporting the existence of the pyridine in the pyridone form in **1** and **3** and the oxypyridine form in **2**. The pyridone and oxypyridine forms in **1–5** were also differentiated by using ¹³C NMR and IR spectroscopic techniques. The pyridone compounds showed a signal at 165–180 ppm in the ¹³C NMR and a peak at ca. 1680 cm⁻¹ in the IR spectra, confirming the presence of a carbonyl carbon. Similar differences in the chemical shifts of the pyrrole and pyridyl protons were also observed for **4** and **5**. However, due to the presence in **4** and **5** of the *meso*-furyl group, which is more in-plane with the BODIPY unit, the pyrrole and pyridyl protons of **4** and **5** were shifted downfield relative to those of the corresponding *meso*-aryl analogues, in which the aryl group is perpendicular to the BODIPY ring. All these above observations clearly suggest that 3,5-bis(oxopyridinyl) substituents alter the π-delocalization of the BODIPY unit more effectively than do 3,5-bis(pyridinyloxy) substituents. These results were also supported by ¹⁹F and ¹¹B NMR spectra. Compounds **1–5** showed characteristic ¹⁹F and ¹¹B NMR signals[10] with a quartet in the ¹⁹F NMR and a triplet in the ¹¹B NMR (Figure 1). In the ¹⁹F NMR spectra, **2** showed a typical quartet at $\delta = -149.1$ ppm, which was shifted downfield for **1** and **3**, appearing at –142.1 ppm in **1** and $\delta = -137.3$ ppm in **3** (Figure S13). Similarly, downfield shifts were also noted in the ¹¹B NMR spectra of **1** and **3** relative to those of **2** (Table 1). Thus, the NMR study revealed that the 3,5-bis(oxopyridinyl)- and 3,5-bis(pyridinyloxy)-BODIPYs showed clear differences in chemical shifts, which is attributed to the differences in the π-delocalization of the BODIPY unit, caused by pyridone and oxypyridine substituents present at the 3- and 5-positions.
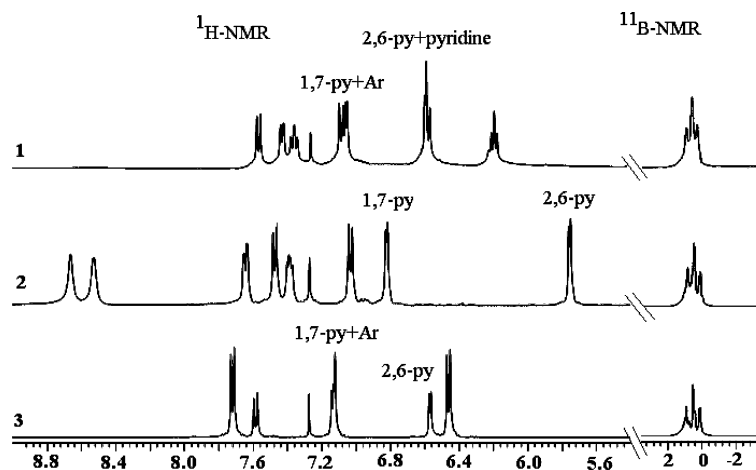
Figure 1. Comparison of ^{1}H and ^{11}B NMR spectra of **1**–**3** in a selected region, recorded in CDCl$_3$.

Table 1. Comparison of ^{1}H, ^{11}B and ^{19}F NMR chemical shift values (in ppm) of **1**–**5**, recorded in CDCl$_3$.

Entry	Compound	^{1}H NMR 2,6-pyrrole	1,7-pyrrole	^{19}F NMR	^{11}B NMR
1	**1**	6.59 (d, J = 3.97 Hz)	7.04 (d, J = 4.27 Hz)	–142.10 (q)	0.61 (t)
2	**2**	5.74 (d, J = 4.27 Hz)	6.81 (d, J = 3.97 Hz)	–149.12 (q)	0.73 (t)
3	**3**	6.56 (d, J = 4.27 Hz)	7.12 (d, J = 3.66 Hz)	–137.29 (q)	0.67 (t)
4	**4**	6.64 (m)	7.56 (d, J = 3.97 Hz)	–142.79 (br. s)	0.56 (t)
5	**5**	7.30 (d, J = 3.97 Hz)	7.62 (m)	–149.26 (q)	0.64 (t)

The absorption properties of **1**–**5** were studied in six different solvents of varying polarity. A comparison of the normalized absorption spectra of **1**–**3** in toluene is shown in part a of Figure 2; **2** and **5** are shown in Figure 2 (b), and the data for **1**–**5** in different solvents are presented in Table 2. Compounds **1**–**5** showed absorption features typical of BODIPYs[4a] such as a strong $S_0{\rightarrow}S_1$ transition at about 520 nm with a vibronic transition on the higher-energy side as a shoulder and an ill-defined, weak band corresponding to the $S_0{\rightarrow}S_2$ transition at about 420 nm. The data presented in Table 2 and Figure 2 reveal the following: (1) the 3,5-bis(4-oxopyridinyl)-BODIPY exhibited an red-shift of about 50 nm in the $S_0{\rightarrow}S_1$ absorption band relative to that of 3,5-bis(2-oxopyridinyl)- and 3,5-bis(3-pyridinyloxy)-BODIPYs. For example, **1** and **2** showed absorption bands at 522 and 518 nm, respectively, whereas **3** showed a 50 nm red-shift in the absorption band and appeared at 569 nm in toluene. This is attributed to the enhancement of π-delocalization in 3,5-bis(4-oxopyridinyl)-BODIPY **3** compared to that of 3,5-bis(2-oxopyridinyl)- and 3,5-bis(3-pyridinyloxy)-BODIPYs **1** and **2**, respectively, (2) the *meso*-furyl analogues showed absorption bands at longer wavelengths compared to that of the corresponding *meso*-aryl analogues (Figure 2, b). For example, the 3,5-bis(pyridinyloxy) *meso*-(4-methoxyphenyl)-BODIPY **2** showed an absorption band at 518 nm in toluene, which is red-shifted in the corresponding *meso*-furyl analogue **5** and appeared at 540 nm. This is due to the in-plane orientation of the *meso*-furyl group and BODIPY unit, which helps increase π-conjugation, unlike the scenario of the *meso*-aryl analogues, in which the *meso*-aryl group is perpendicular to the BODIPY

ring and restricts conjugation, (3) the absorption band of 3,5-bis(3-pyridinyloxy)-BODIPYs **2** and **5** is narrower with full-width at half-maximum (FWHM) values in the range of 800–1405 cm^{-1} in toluene, whereas the absorption band of 3,5-bis(2/4-oxopyridinyl)-BODIPYs **1**, **3** and **4** is very broad, with FWHM values of 1450–2530 cm^{-1} in toluene, (4) the *meso*-furyl analogues exhibit broader absorption bands than do the *meso*-aryl analogues and (5) the absorption of **1** in different solvents shown in Figure 3 indicates that **1**–**5** exhibit a blueshift in the absorption band and an increase in the FWHM with increasing solvent polarity,[11] and maximum solvent effects were noted for 3,5-bis(oxopyridinyl)-BODIPYs. Thus, the absorption studies reveal that 3,5-bis(oxopyridinyl)-BODIPYs showed broad, red-shifted $S_0{\rightarrow}S_1$ absorption bands, whereas the 3,5-bis(pyridinyloxy)-BODIPYs exhibited narrow, well-defined absorption bands with absorption features matching other BODIPYs reported in the literature.[3] Furthermore, the *meso*-furyl-BODIPYs showed broad and red-shifted absorption bands compared to those of the *meso*-anisyl analogues.

The electrochemical properties of 3,5-bis(2/4-oxopyridinyl)- and 3,5-bis(3-pyridinyloxy)-BODIPYs **1**–**5** were determined by cyclic voltammetry at a scan rate of 50 mV/s using tetrabutylammonium perchlorate (TBAP) as the supporting electrolyte. A comparison of the reduction waves of **1**–**3** is shown in Figure 4 (a), and the reduction waves of **2** and **5** are shown in Figure 4 (b). The redox potential data for **1**–**5** are presented in Table 3. Compounds **1**–**5** showed one oxidation and two reductions occurring at the BODIPY unit. The oxidation and one of the reduction are irreversible and did not follow any definite trend. However, the first re-
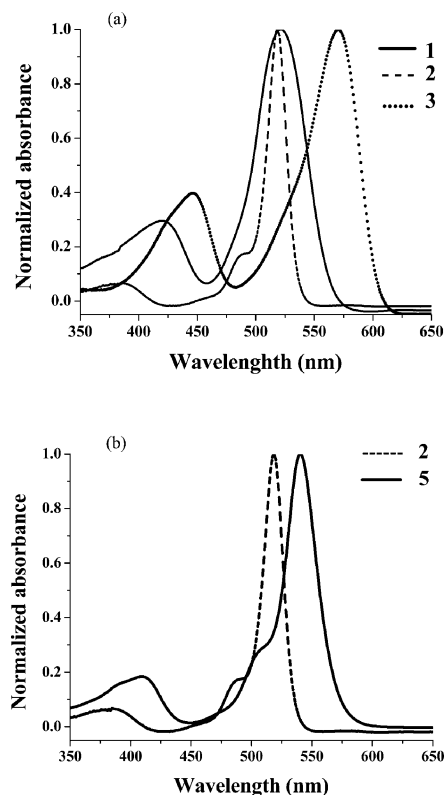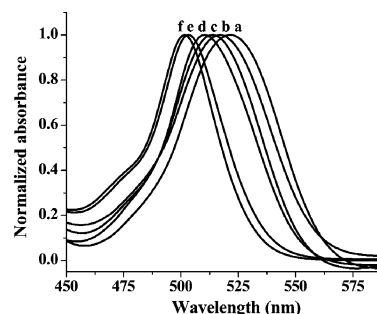
Figure 3. Comparison of normalized absorption spectra of **1**, recorded in (a) toluene; (b) THF; (c) EtOAc; (d) CHCl$_3$; (e) MeCN and (f) MeOH.

duction is quasireversible and exhibited a systematic trend with the substituents present at the 3- and 5-positions as well as at the *meso*-position. An inspection of Figure 4 (a, b) and the data presented in Table 3 reveal the following: (1) the first reduction potentials of 3,5-bis(oxopyridinyl)-BODIPYs were less negative than those of 3,5-bis(pyridinyloxy)-BODIPYs by 200–400 mV, indicating that 3,5-bis(oxopyridinyl)-BODIPYs are easier to reduce than 3,5-bis(pyridinyloxy)-BODIPYs, (2) the 3,5-disubstituted *meso*-furyl-BODIPYs are easier to reduce than the corresponding 3,5-disubstituted *meso*-aryl-BODIPYs and (3) among 3,5-bis-(2/4-oxopyridinyl)-BODIPYs, the 3,5-bis(4-oxopyridinyl)-BODIPY **3** exhibited a less negative reduction potential

Figure 2. Comparison of normalized absorption spectra of (a) **1–3** and (b) **2** and **5**, recorded in toluene.

Table 2. Photophysical properties of BODIPYs **1–5** in different solvents. * Broad, ill-defined band.

Entry	Compd.	Solvent	λ_{abs} [nm]	λ_{em} [nm]	FWHM (abs.) [cm^{-1}]	$\Delta\nu_{st}$ [cm^{-1}]	ε	ϕ	τ [ns]	$k_f 10^8$	$k_{nr} 10^9$
1	**1**	toluene	522	569	2530	1570	4.48	0.063	0.77	0.81	1.21
2		CHCl$_3$	510	567	1870	1640	4.45	0.027	0.46	0.58	2.11
3		THF	518	566	1910	1650	4.48	0.019	0.30	0.63	3.21
4		EtOAc	512	560	1980	1680	4.49	0.028	0.26	1.07	3.73
5		MeOH	501	537	1570	1310	4.61	0.0036	0.12	0.30	8.3
6		MeCN	503	549	1450	1650	4.62	<0.001	–	–	–
7	**2**	toluene	518	531	810	450	4.94	0.45	2.13	2.11	7.8
8		CHCl$_3$	516	531	1090	510	4.91	0.58	2.58	2.24	1.6
9		THF	514	529	1000	550	4.87	0.33	1.30	2.53	5.1
10		EtOAc	512	528	950	570	4.93	0.286	1.46	1.95	4.8
11		MeOH	510	523	950	460	4.89	0.23	1.37	1.67	5.6
12		MeCN	510	526	1070	570	4.79	0.25	1.08	2.31	6.9
13	**3**	toluene	569	600	1930	910	4.69	0.30	1.43	2.09	4.8
14		CHCl$_3$	548	584	1980	1130	4.69	0.175	1.01	1.73	8.1
15		THF	555	591	1700	1110	4.63	0.055	0.59	0.93	1.6
16		EtOAc	551	587	1930	1110	4.7	0.078	0.58	1.34	1.58
17		MeOH	485	535	4270*	1900	4.39	0.022	0.18	1.22	5.4
18		MeCN	534	576	2210	1370	4.67	0.025	0.22	1.13	4.4
19	**4**	toluene	550	625	2240	2181	4.12	0.027	1.37	0.19	0.71
20		CHCl$_3$	536	624	2107	2646	4.47	0.023	1.07	0.21	0.91
21		THF	543	632	2177	2606	4.21	0.0083	0.50	0.16	1.98
22		EtOAc	539	621	2104	2449	4.51	0.0063	0.47	0.13	2.11
23		MeOH	528	607	1932	2465	4.52	0.002	–	–	–
24		MeCN	525	600	1819	2381	4.46	0.0013	–	–	–
25	**5**	toluene	540	589	1405	1541	4.79	0.169	2.9	0.58	2.8
26		CHCl$_3$	538	583	1206	1449	4.56	0.15	3.3	0.45	2.5
27		THF	535	583	1409	1553	4.84	0.115	2.4	0.48	3.6
28		EtOAc	533	580	1292	1523	4.72	0.10	2.27	0.44	3.9
29		MeOH	530	575	1217	1480	4.82	0.111	2.21	0.50	4.0
30		MeCN	531	578	1290	1543	4.79	0.119	2.14	0.55	4.1

than that of 3,5-bis(2-oxopyridinyl)-BODIPY **1**, indicating that **3** is much easier to reduce than **1**. Thus, the electrochemical study clearly indicated that the *meso*-furyl-BODIPYs were easier to reduce than the corresponding *meso*-anisyl analogues. Furthermore, the electron-withdrawing 2- and 4-pyridone substituents at the 3- and 5-positions render the reduction of these compounds more facile than that of 3,5-bis(3-pyridinyloxy)-BODIPYs. The 3,5-bis(4-oxopyridinyl)-BODIPY is much easier to reduce than the 3,5-bis(2-oxopyridinyl)-BODIPY, suggesting that the 3,5-bis(4-oxopyridinyl)-BODIPYs are more stable towards reduction than are the 3,5-bis(2-oxopyridinyl)-BODIPYs.
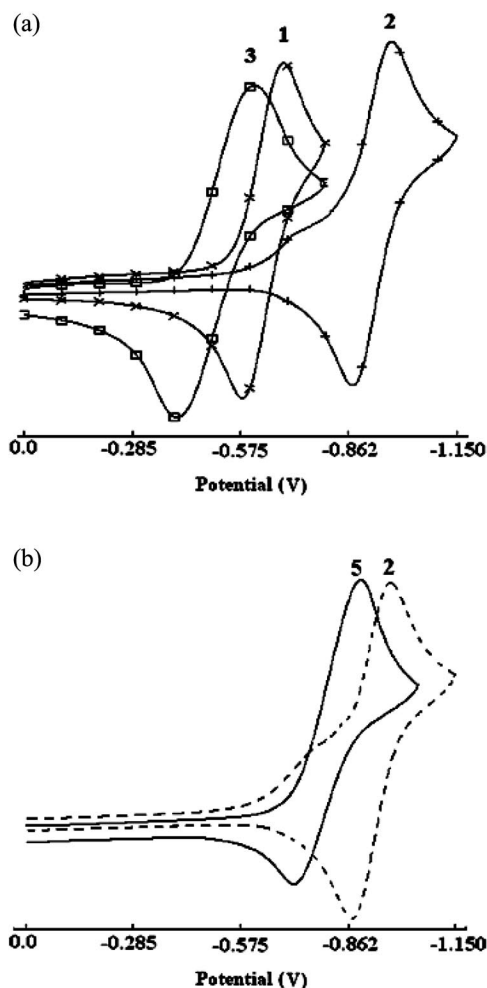
Table 3. Electrochemical redox data [V] of **1**–**5** in CH$_2$Cl$_2$ containing 0.1 M TBAP as the supporting electrolyte.

Entry	Compound	Oxidation	Reduction	
			I	II
1	**1**	–	–0.626	–1.71
2	**2**	1.28	–0.913	–1.53
3	**3**	1.48	–0.504	–1.54
4	**4**	1.66	–0.460	–1.50
5	**5**	1.25	–0.789	–1.69

Figure 4. Comparison of reduction waves of cyclic voltammograms of (a) **1**–**3** and (b) **2** and **5** in CH$_2$Cl$_2$ containing 0.1 M TBAP as the supporting electrolyte recorded at a scan speed of 50 mV/sec.

The fluorescence properties of **1**–**5** were studied in six different solvents by steady-state and time-resolved fluorescence techniques (Table 2). The steady-state fluorescence studies on **1**–**5** reveal the following: (1) all the compounds (**1**–**5**) showed one single emission band, and the band width depended on the kind of substituents present at the 3- and 5-positions as well as at the *meso*-position, (2) the 3,5-bis(oxopyridinyl)-BODIPYs showed emission bands bathochromically shifted with respect to those of the 3,5-bis(pyr-

idinyloxy)-BODIPYs. For example, among **1**–**3**, the 3,5-bis(pyridinyloxy)-BODIPY **2** showed an emission band at 531 nm, and the 3,5-bis(2/4 pyridone)-BODIPYs **1** and **3** showed red-shifted emission bands at 569 and 600 nm, respectively [Figure 5 (a)], (3) the 3,5-bis(pyridinyloxy)-BODIPYs showed narrow emission bands, whereas the emission band of 3,5-bis(2/4 pyridone)-BODIPYs are much broader, (4) among 3,5-bis(oxopyridinyl) derivatives such as **1** and **3**, **3** showed a broad and red-shifted emission band compared to that of **1**. This is attributed to an extension of π-delocalization in **3**, (5) the *meso*-furyl-BODIPYs exhibited broad and red-shifted emission bands compared to those of the corresponding *meso*-aryl-BODIPYs, (6) the quantum yields of 3,5-bis(pyridinyloxy)-BODIPYs are relatively higher than those of the 3,5-bis(oxopyridinyl)-BODIPYs, and the *meso*-furyl derivatives showed lower emission yields compared to that of their corresponding *meso*-anisyl derivatives (Table 2), (7) **1**–**5** showed slight hypochromic shifts with a reduction in the quantum yield upon increasing solvent polarity, which is consistent with the general behaviour of BODIPY compounds[11] and (8) the 3,5-bis(pyridinyloxy)-BODIPYs showed a slight Stokes shift (12 nm), as shown in part b of Figure 5 for **2**, whereas the 3,5-bis(2/4-oxopyridinyl)-BODIPYs exhibited much larger Stokes shift (ca. 50 nm), as shown in Figure 5 (c) for **1**. Moreover, the Stokes shifts of each compound do not vary much as a function of the solvent. These observations indicate that the structures of 3,5-bis(oxopyridinyl)-BODIPYs in the ground state and excited state are different from each other unlike with the 3,5-bis(pyridinyloxy)-BODIPYs, which may possess the same structure in the ground and excited states. Thus, the Stokes shift data indicate that 3,5-bis(oxopyridinyl)-BODIPYs undergo structural reorganization in the excited state.

Time-resolved studies were carried out on **1**–**5** to understand their fluorescence properties in detail, and a representative fluorescence decay of **2** is shown in Figure 5 (d). Compounds **1**–**5** generally showed a single exponential decay in all solvents, and the lifetimes parallel the fluorescence quantum yields. The 3,5-bis(pyridinyloxy)-BODIPYs exhibited longer singlet-state lifetimes than that of the 3,5-bis(oxopyridinyl)-BODIPYs. These observations are consistent with the observed fluorescence yields. The decrease in k_f and increase in k_{nr} are in agreement with the shorter lifetimes of the 3,5-bis(oxopyridinyl)-BODIPYs compared to that of the 3,5-bis(pyridinyloxy)-BODIPYs. Thus, the relatively low fluorescence yields observed for 3,5-bis(oxopyridinyl)-BODIPYs may be due to the decreased S$_1$ state life-
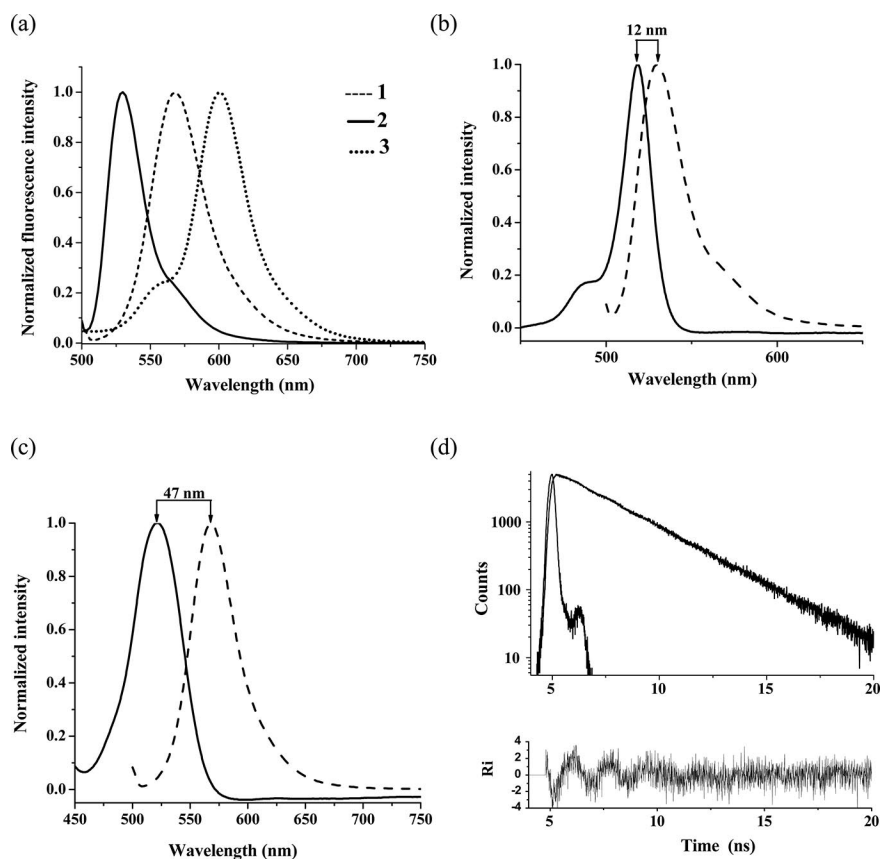
(a)

(b)

(c)

(d)

Figure 5. (a) Comparison of normalized emission spectra of **1**–**3**, recorded in toluene, at λ_{ex} = 488 nm (b) Comparision of normalized absorption (−) and emission (---) spectra of 3,5-bis(pyridinyloxy) **2** in toluene. (c) Comparision of normalized absorption (−) and emission (---) spectra of 3,5-bis(oxopyridinyl) **1** in toluene. (d) Fluorescence decay profile and weighted, residual, distribution fit of **2** in chloroform. The excitation wavelength used was 406 nm and emission was detected at 531 nm.

time and possibly due to the increased $S_1{\rightarrow}T_1$ intersystem crossing and increased $S_1{\rightarrow}S_0$ internal conversion rates. The large Stokes shifts observed for the 3,5-bis(oxopyridinyl)-BODIPYs support the enhancement of the Franck–Condon factor due to substantial structural reorganization in the excited state, resulting in the increased nonradiative decay rates.

Conclusions

We have described the synthesis of 3,5-bis(oxopyridinyl)-BODIPYs and 3,5-bis(pyridinyloxy)-BODIPYs by reacting the corresponding 3,5-dibromo-BODIPYs with 2-, 3- and 4-hydroxypyridines in MeCN in the presence of Cs_2CO_3. The absorption studies indicated that the 3,5-bis(oxopyridinyl)-BODIPYs exhibit broad, red-shifted absorption bands relative to those of the 3,5-bis(pyridinyloxy)-BODIPYs. The presence of the *meso*-furyl group also induces red-shifts in the absorption bands relative to those of the *meso*-anisyl analogues. The electrochemical study revealed that the 3,5-bis(oxopyridinyl)-BODIPYs are easier to reduce than the 3,5-bis(oxypridine)-BODIPYs, supporting the electron-deficient nature of pyridone groups. The fluorescence study indicated that the 3,5-bis(oxopyridinyl)-BODIPYs exhibit a broad, red-shifted, emission bands with low quantum yields

and singlet-state lifetimes relative to those of the 3,5-bis-(pyridinyloxy)-BODIPYs. All these results suggest that the electronic properties of a BODIPY dye depend on the kind of substituents (pyridine versus oxypyridine) present at the 3- and 5-positions. We believe that the remarkable differences in the spectral, electrochemical and photophysical properties between 3,5-bis(oxopyridinyl)-BODIPYs and 3,5-bis(pyridinyloxy)-BODIPYs will lead to a wide range of applications in biological and molecular sensors.

Experimental Section

Chemicals: THF and toluene were dried with sodium benzophenone ketyl, and $CHCl_3$, EtOAc, CH_3OH and MeCN were dried with calcium hydride and distilled prior to use. $BF_3{\cdot}OEt_2$ and DDQ were obtained from Spectrochem (India) and used as obtained. All other chemicals used for the synthesis were reagent-grade unless otherwise specified. Column chromatography was performed on silica (60–120 mesh).

Instrumentation: ^{1}H NMR spectra (δ values, ppm) were recorded using Varian VXR 300 and 400 MHz spectrometers. ^{13}C NMR spectra were recorded with a Varian spectrometer operating at 100.6 MHz. ^{19}F NMR spectra were recorded with a Varian spectrometer operating at 282.2 MHz. ^{11}B NMR spectra were recorded with a Varian spectrometer operating at 96.3 MHz. Tetramethylsilane (TMS) was used as an external reference for recording [1]H (of

residual proton; δ = 7.26 ppm) and ^{13}C (δ = 77.0 ppm) spectra in CDCl$_3$. Absorption and steady-state fluorescence spectra were obtained with a Perkin–Elmer Lambda-35 spectrometer and a PC1 Photon Counting Spectrofluorimeter (ISS, USA). Fluorescence spectra were recorded at 25 °C in a 1-cm quartz fluorescence cuvette. The fluorescence quantum yields (Φ_f) were estimated from the emission and absorption spectra by the comparative method at the excitation wavelength of 488 nm using Rhodamine 6G (Φ_f = 0.88)[7h] as the standard. The time-resolved fluorescence decay measurements were carried out at the magic angle using a picosecond-diode-laser-based, time-correlated, single-photon-counting (TCSPC) fluorescence spectrometer[9] from IBH, UK. All the decays were fitted to a single exponential.

Cyclic voltammetric (CV) and differential pulse voltammetric (DPV) studies were carried out with an electrochemical system utilizing a three-electrode configuration consisting of a glassy carbon (working) electrode, platinum wire (auxiliary) electrode and a saturated calomel (reference) electrode.[9] The experiments were performed in dry CH$_2$Cl$_2$ using 0.1 M TBAP as the supporting electrolyte. Half-wave potentials were measured using DPV and also calculated manually by taking the average of the cathodic and anodic peak potentials. MALDI-TOF spectra were obtained with an Axima-CFR spectrometer, manufactured by Kratos Analyticals. LC-MS spectra were obtained with a Varian Pro Star 500 MS.

2,10-Dibromo-*meso*-(4-methoxyphenyl)dipyrromethane (8): *meso*-(4-Methoxyphenyl)dipyrromethane (**7**, 1.0 g, 4.23 mmol) in dry THF (75 mL) was cooled to –78 °C under an argon atmosphere and treated with *N*-bromosuccinimide (1.6 g, 9.0 mmol) for 1 h. The reaction mixture was brought to room temperature, and the solvent was removed in a rotary evaporator under vacuum. The crude compound was purified by silica gel column chromatography using petroleum ether and afforded pure **8** as a red solid in 75% yield (1.27 g); m.p. 118–119 °C. ^{1}H NMR (400 MHz, CDCl$_3$): δ = 3.9 (s, 3 H, -OCH$_3$), 5.29 (s, 1 H, -CH), 5.82 (m, 2 H, pyrrole), 6.06 (m, 2 H, pyrrole), 7.06 (d, J = 7.8 Hz, 2 H, Ar), 7.13 (d, J = 7.8 Hz, 2 H, Ar) ppm. C$_{16}$H$_{14}$Br$_2$N$_2$O (410.11): calcd. C 46.86, H 3.44, N 6.83; found C 47.02, H 3.53, N 6.95.

3,5-Dibromo-4,4-difluoro-8-(4-methoxyphenyl)-4-bora-3a,4a-diaza-*s*-indacene (9): Compound **8** (500 mg, 1.31 mmol) in CH$_2$Cl$_2$ (30 mL) was oxidized with DDQ (300 mg, 1.31 mmol) at room temperature whilst being stirred for 1 h. Et$_3$N (6.4 mL) was added, followed by BF$_3$·OEt$_2$ (8.20 mL, 65.8 mmol), and stirring was continued at room temperature for an additional 1 h. The reaction mixture was washed successively with aqueous NaOH (0.1 M) and water thoroughly. The combined organic layers were dried with Na$_2$SO$_4$ and filtered, and the solvents were evaporated. The crude product was purified by silica gel column chromatography using CH$_2$Cl$_2$ and afforded **9** as an orange-red powder in 25% yield (208 mg); m.p. 210–211 °C. ^{1}H NMR (400 MHz, CDCl$_3$): δ = 3.9 (s, 3 H, -OCH$_3$), 6.52 (d, J = 4.28 Hz, 2 H, pyrrole), 6.82 (d, J = 4.28 Hz, 2 H, pyrrole), 7.01 (d, J = 7.9 Hz, 2 H, Ar), 7.42 (d, J = 7.9 Hz, 2 H, Ar) ppm. ^{13}C NMR (100 MHz, CDCl$_3$): δ = 55.63, 114.27, 122.56, 124.87, 131.60, 131.87, 132.33, 135.48, 148.42, 162.22 ppm. ^{19}F NMR (282.2 MHz, CDCl$_3$): δ = –147.09 (q, $J_{B,F}$ = 57.8 Hz) ppm. ^{11}B NMR (96.3 MHz, CDCl$_3$): δ = 0.88 (t, $J_{B,F}$ = 28.2 Hz) ppm. MALDI-TOF: m/z = 454.5 [M]$^+$. C$_{16}$H$_{11}$BBr$_2$F$_2$N$_2$O (455.89): calcd. C 42.15, H 2.43, N 6.14; found C 42.87, H 2.62, N 6.45.

meso-(2-Furyl)dipyrromethane (10): In a 250 mL, round-bottomed flask, freshly distilled furfural (1 g, 8.97 mmol) and pyrrole (15.5 mL, 0.22 mmol) were dissolved in CH$_2$Cl$_2$ (50 mL) under an argon atmosphere. BF$_3$·OEt$_2$ (123 µL, 0.89 mmol) was added to ini-

tiate the reaction, and the reaction mixture was stirred for 15 min at room temperature. The reaction mixture was diluted with CH$_2$Cl$_2$ and washed thoroughly with aqueous NaOH (0.1 M) and water. The organic layers were combined, dried with Na$_2$SO$_4$ and concentrated in a rotary evaporator. The crude compound was subjected to silica gel column and afforded pure *meso*-(2-furyl)dipyrromethane **10** using petroleum ether/EtOAc (95:5) as a white solid in 63% yield (1.2 g); m.p. 120 °C. ^{1}H NMR (400 MHz, CDCl$_3$): δ = 5.49 (s, 1 H, furan), 5.98 (s, 2 H, pyrrole), 6.12–6.15 (m, 2 H, pyrrole), 6.31–6.33 (m, 1 H, furan), 6.67 (d, J = 1.52 Hz, 2 H, pyrrole), 7.38 (s, 1 H, furan), 8.04 (br. s, 2 H, NH) ppm. ^{13}C NMR (100 MHz, CDCl$_3$): δ = 37.7, 37.8, 106.7, 106.8, 106.9, 108.1, 108.3, 110.3, 117.6, 117.7, 129.9, 142.0, 154.4 ppm. LC-MS: m/z = 211.2 [M]$^+$. C$_{13}$H$_{12}$N$_2$O (212.25): calcd. C 73.56, H 5.70, N 13.20; found C 73.92, H 5.95, N 13.56.

2,10-Dibromo-*meso*-(2-furyl)dipyrromethane (11): *meso*-(2-Furyl)dipyrromethane **10** (1.0 g, 4.71 mmol) was treated with *N*-bromosuccinimide (1.67 g, 9.4 mmol) in THF at –78 °C under an argon atmosphere for 1 h, and the resulting crude compound was purified by silica gel column chromatograhy using petroleum ether to afford pure **11** as a dark solid in 73% yield (1.4 g); m.p. 118–119 °C. ^{1}H NMR (400 MHz, CDCl$_3$): δ = 5.39 (s, 1 H, CH), 5.91 (s, 2 H, furan), 6.09 (s, 2 H, pyrrole), 6.16 (s, 1 H, pyrrole), 6.35 (s, 1 H, pyrrole), 7.41 (s, 1 H, furan), 7.99 (s, 1 H, furan), 8.27 (br. s, 2 H, NH) ppm. ^{13}C NMR (100 MHz CDCl$_3$): δ = 29.7, 36.7, 38.0, 90.3, 97.8, 107.5, 109.0, 110.5, 110.6, 130.8, 142.6, 149.5, 178.8 ppm. LC-MS: m/z = 375.6 [M]$^+$. C$_{13}$H$_{10}$Br$_2$N$_2$O (370.04): calcd. C 42.20, H 2.72, N 7.57; found C 42.43, H 2.89, N 7.92.

3,5-Dibromo-4,4-difluoro-8-(2-furyl)-4-bora-3a,4a-diaza-*s*-indacene (12): Compound **11** (0.500 g, 1.35 mmol) in CH$_2$Cl$_2$ was first oxidized with DDQ (306 mg, 1.35 mmol) at room temperature for 1 h. The reaction mixture was then treated with a small amount of Et$_3$N (6.6 mL) followed by BF$_3$·OEt$_2$ (9.3 mL, 67.5 mmol), and the mixture was stirred for an additional 1 h at room temperature. The solvent was removed in a rotary evaporator, and the resultant crude compound was purified by silica gel column chromatography using CH$_2$Cl$_2$ as the eluent. Pure **12** was obtained as dark-red solid in 42% yield (375 mg). ^{1}H NMR (400 MHz, CDCl$_3$): δ = 6.58 (d, J = 3.97 Hz, 2 H, pyrrole), 6.70 (m, 1 H, furan), 7.10 (d, J = 3.66 Hz, 1 H, furan), 7.33 (d, J = 4.27 Hz, 2 H, pyrrole), 7.83 (s, 1 H, furan) ppm. ^{13}C NMR (100 MHz CDCl$_3$): δ = 113.5, 120.3, 122.7, 129.2, 131.0, 131.6, 133.2, 147.5, 147.8 ppm. LC-MS: m/z = 397.0 [M – 19]$^+$. C$_{13}$H$_8$BBr$_2$F$_2$N$_2$O (416.83): calcd. C 37.46, H 1.93, N 6.72; found C 37.78, H 2.01, N 6.89.

General Synthetic Procedure for the Preparation of 3,5-Dipyridone and 3,5-Dioxypyridine-substituted Boron-dipyrromethenes 1–5: Compounds **1**–**5** were synthesized by treating the corresponding 3,5-dibromo dipyrromethene **9** or **12** (1 equiv.) with 2-, 3- or 4-hydroxypyridine (3 equiv.) in MeCN in the presence of Cs$_2$CO$_3$ (2.5 equiv.) under an inert atmosphere at reflux for 1 h. The progress of the reaction was followed by TLC analysis, which showed the disappearance of the starting compound and appearance of a new spot corresponding to the desired compound. The solvent was removed in a rotary evaporator under vacuum, and the crude compound was subjected to silica gel column chromatography using CH$_2$Cl$_2$/2–5% CH$_3$OH.

3,5-Bis(1,2-dihydro-2-oxopyridin-1-yl)-4,4-difluoro-8-(4-methoxyphenyl)-4-bora-3a,4a-diaza-*s*-indacene (1): Compound **1** was obtained as a red solid in 75% yield. ^{1}H NMR (400 MHz, CDCl$_3$): δ = 3.92 (s, 3 H, -OCH$_3$), 6.17 (t, J_1 = J_2 = 6.72 Hz, 2 H, pyridine), 6.54 (m, 2 H, pyridine), 6.59 (d, J = 3.97 Hz, 2 H, pyrrole), 7.04 (d, J = 4.27 Hz, 2 H, pyrrole), 7.07 (d, J = 8.55 Hz, 2 H, Ar), 7.33

(m, 2 H, pyridine), 7.42 (d, J = 6.72 Hz, 2 H, pyridine), 7.55 (d, J = 8.55 Hz, 2 H, Ar) ppm. ^{13}C NMR (100 MHz, CDCl$_3$): δ = 55.53, 102.98, 114.07, 124.45, 125.31, 127.65, 128.36, 130.80, 132.04, 142.32, 146.83, 161.54, 162.64 ppm. ^{19}F NMR (282.2 MHz, CDCl$_3$): δ = –142.10 (q, $J_{B,F}$ = 60.9 Hz) ppm. ^{11}B NMR (96.3 MHz, CDCl$_3$): δ = 0.61 (t, $J_{B,F}$ = 28.9 Hz) ppm. IR (KBr film): $\tilde{\nu}$ = 1681 cm^{-1}. MALDI-TOF: m/z = 463.8 [M – 19]$^+$. C$_{26}$H$_{19}$BF$_2$N$_4$O$_3$ (484.27): calcd. C 64.49, H 3.95, N 11.57; found C 65.12, H 4.09, N 11.96.

4,4-Difluoro-8-(4-methoxyphenyl)-3,5-bis(pyridin-3-yloxy)-4-bora-3a,4a-diaza-s-indacene (2): Compound **2** was obtained as a green solid in 70% yield. ^{1}H NMR (400 MHz, CDCl$_3$): δ = 3.89 (s, 3 H, -OCH$_3$), 5.74 (d, J = 4.27 Hz, 2 H, pyrrole), 6.81 (d, J = 3.97 Hz, 2 H, pyrrole), 7.02 (d, J = 8.55 Hz, 4 H, Ar), 7.36 (q, J = 4.58 Hz, 2 H, pyridine), 7.46 (d, J = 8.55 Hz, 2 H, Ar), 7.63 (d, J = 7.02 Hz, 2 H, pyridine), 8.52 (s, 2 H, pyridine), 8.66 (s, 2 H, pyridine) ppm. ^{13}C NMR (100 MHz, CDCl$_3$): δ = 55.89, 114.32, 114.83, 119.02, 124.93, 133.16, 139.26, 148.70, 152.02, 163.26, 179.28 ppm. ^{19}F NMR (282.2 MHz, CDCl$_3$): δ = –149.12 (q, $J_{B,F}$ = 55.0 Hz) ppm. ^{11}B NMR (96.3 MHz, CDCl$_3$): δ = 0.73 (t, $J_{B,F}$ = 27.4 Hz) ppm. MALDI-TOF: m/z = 483.7 [M]$^+$. C$_{26}$H$_{19}$BF$_2$N$_4$O$_3$ (484.27): calcd. C 64.49, H 3.95, N 11.57; found C 65.17, H 4.12, N 11.92.

3,5-Bis(1,4-dihydro-4-oxopyridin-1-yl)-4,4-difluoro-8-(4-methoxyphenyl)-4-bora-3a,4a-diaza-s-indacene (3): Compound **3** was obtained as a red fluorescent solid in 66% yield. ^{1}H NMR (400 MHz, CDCl$_3$): δ = 3.95 (s, 3 H, -OCH$_3$), 6.45 (d, J = 7.94 Hz, 4 H, pyridine), 6.56 (d, J = 4.27 Hz, 2 H, pyrrole), 7.12 (m, 4 H, Ar, pyrrole), 7.57 (d, J = 8.55 Hz, 2 H, Ar), 7.70 (d, J = 7.63 Hz, 4 H, pyridine) ppm. ^{13}C NMR (100 MHz, CDCl$_3$): δ = 55.8, 114.3, 114.8, 119.0, 124.9, 133.1, 139.2, 148.7, 152.0, 163.2, 179.2 ppm. ^{19}F NMR (282.2 MHz, CDCl$_3$): δ = –137.29 (q, $J_{B,F}$ = 60.9 Hz) ppm. ^{11}B NMR (96.3 MHz, CDCl$_3$): δ = 0.67 (t, $J_{B,F}$ = 28.9 Hz) ppm. IR (KBr film): $\tilde{\nu}$ = 1640 cm^{-1}. MALDI-TOF: m/z = 484.5 [M]$^+$. C$_{26}$H$_{19}$BF$_2$N$_4$O$_3$ (484.27): calcd. C 64.49, H 3.95, N 11.57; found C 65.15, H 4.04, N 11.69.

3,5-Bis(1,2-dihydro-2-oxopyridin-1-yl)-4,4-difluoro-8-(2-furyl)-4-bora-3a,4a-diaza-s-indacene (4): Compound **4** was obtained as a red solid in 46% yield. ^{1}H NMR (400 MHz, CDCl$_3$): δ = 6.18 (m, 2 H, pyridine), 6.57 (d, J = 9.77 Hz, 2 H, pyridine), 6.64 (m, 2 H, pyrrole), 6.78 (s, 1 H, furan), 7.35 (m, 5 H, pyridine, furan), 7.56 (d, J = 3.97 Hz, 2 H, pyrrole), 7.91 (d, J = 1.83 Hz, 1 H, furan) ppm. ^{19}F NMR (282.2 MHz, CDCl$_3$): δ = –142.79 (br. s) ppm. ^{11}B NMR (96.3 MHz, CDCl$_3$): δ = 0.56 (t, $J_{B,F}$ = 28.9 Hz) ppm. MALDI-TOF: m/z = 423.9 [M – 19]$^+$. C$_{23}$H$_{15}$BF$_2$N$_4$O$_3$ (444.20): calcd. C 62.19, H 3.40, N 12.61; found C 62.53, H 3.56, N 12.75.

4,4-Difluoro-8-(2-furyl)-3,5-bis(3-pyridin-3-yloxy)-4-bora-3a,4a-diaza-s-indacene (5): Compound **5** was obtained as green, crystalline solid in 62% yield. ^{1}H NMR (400 MHz, CDCl$_3$): δ = 5.79 (d, J = 4.27 Hz, 2 H, pyridine), 6.65 (m, 1 H, furan), 6.97 (d, J = 3.66 Hz, 1 H, furan), 7.30 (d, J = 3.97 Hz, 2 H, pyrrole), 7.36 (q, J = 4.88 Hz, 2 H, pyridine), 7.62 (m, 2 H, pyrrole), 7.75 (s, 1 H, furan), 8.52 (d, J = 4.58 Hz, 2 H, pyridine), 8.65 (d, J = 2.44 Hz, 2 H, pyridine) ppm. ^{13}C NMR (100 MHz, CDCl$_3$): δ = 102.8, 112.4, 117.2, 124.18, 124.5, 126.0, 127.3, 127.7, 130.2, 142.1, 142.5, 146.0, 146.7, 151.4, 162.2 ppm. ^{19}F NMR (282.2 MHz, CDCl$_3$): δ = –149.26 (q, $J_{B,F}$ = 55.0 Hz) ppm. ^{11}B NMR (96.3 MHz, CDCl$_3$): δ = 0.64 (t, $J_{B,F}$ = 27.4 Hz) ppm. MALDI-TOF: m/z = 443.8 [M]$^+$. C$_{23}$H$_{15}$BF$_2$N$_4$O$_3$ (444.20): calcd. C 62.19, H 3.40, N 12.61; found C 62.76, H 3.62, N 12.89.

Supporting Information (see also the footnote on the first page of this article): ^{1}H, ^{13}C and ^{19}F NMR spectra and mass spectra of all compounds.

[1] A. Kocak, S. Kurbanli, *Synth. Commun.* **2007**, *37*, 3697–3708 and references cited therein.

[2] For recent reviews, see: a) R. Ziessel, G. Ulrich, A. Harriman, *New J. Chem.* **2007**, *31*, 496–501; b) A. Loudet, K. Burgess, *Chem. Rev.* **2007**, *107*, 4891–4932; c) G. Ulrich, R. Ziessel, A. Harriman, *Angew. Chem. Int. Ed.* **2008**, *47*, 1184–1201.

[3] a) M. Kollmannsberger, K. Rurack, U. Resch-Genger, J. Daub, *J. Phys. Chem. A* **1998**, *102*, 10211–10220; b) T. López Arbeloa, F. López Arbeloa, I. López Arbeloa, I. García-Moreno, A. Costela, R. Sastre, F. Amat-Guerri, *Chem. Phys. Lett.* **1999**, *299*, 315–321; c) K. Rurack, M. Kollmannsberger, J. Daub, *Angew. Chem. Int. Ed.* **2001**, *40*, 385–387; d) B. Cunderlikova, L. Sikurova, *Chem. Phys.* **2001**, *263*, 415–422; e) R. Y. Lai, A. J. Bard, *J. Phys. Chem. B* **2003**, *107*, 5036–5042; f) W. Qin, M. Baruah, A. Stefan, M. Van der Auweraer, N. Boens, *ChemPhysChem* **2005**, *6*, 2343–2351; g) W. Qin, M. Baruah, M. Van der Auweraer, F. C. De Schryver, N. Boens, *J. Phys. Chem. A* **2005**, *109*, 7371–7384; h) T. Rohand, W. Qin, N. Boens, W. Dehaen, *Eur. J. Org. Chem.* **2006**, 4658–4663; i) M. Baruah, W. Qin, C. Flors, J. Hofkens, R. A. L. Vallée, M. Van der Auweraer, W. M. De Borggraeve, N. Boens, *J. Phys. Chem. A* **2006**, *110*, 5998–6009; j) A. C. Benniston, G. Copley, K. J. Elliott, R. W. Harrington, W. Clegg, *Eur. J. Org. Chem.* **2008**, 2705–2713; k) M. Bröring, R. Krüger, S. Link, C. Kleeberg, S. Köhler, X. Xie, B. Ventura, L. Flamigni, *Chem. Eur. J.* **2008**, *14*, 2976–2983; l) W. Qin, M. Baruah, M. Sliwa, M. Van der Auweraer, W. M. De Borggraeve, D. Beljonne, B. Van Averbeke, N. Boens, *J. Phys. Chem. A* **2008**, *112*, 6104–6114; m) B. Ventura, G. Marconi, M. Bröring, R. Krüger, L. Flamigni, *New J. Chem.* **2009**, *33*, 428–438; n) K. Guzow, K. Kornowska, W. Wiczk, *Tetrahedron Lett.* **2009**, *50*, 2908–2910; o) E. Fron, E. Coutiño-Gonzalez, L. Pandey, M. Sliwa, M. Van der Auweraer, F. C. De Schryver, J. Thomas, Z. Dong, V. Leen, M. Smet, W. Dehaen, T. Vosch, *New J. Chem.* **2009**, *33*, 1490–1496.

[4] a) H. L. Kee, C. Kirmaier, L. Yu, P. Thamyongkit, W. J. Youngblood, M. E. Calder, L. Ramos, B. C. Noll, D. F. Bocian, W. R. Scheidt, R. R. Birge, J. S. Lindsey, D. Holten, *J. Phys. Chem. B* **2005**, *109*, 20433–20443; b) E. Lager, J. Liu, A. Aguilar-Aguilar, B. Z. Tang, E. Peña-Cabrera, *J. Org. Chem.* **2009**, *74*, 2053–2058.

[5] a) M. Baruah, W. Qin, R. A. L. Vallée, D. Belijonne, T. Rohand, W. Dehaen, N. Boens, *Org. Lett.* **2005**, *7*, 4377–4380; b) T. Rohand, M. Baruah, W. Qin, N. Boens, W. Dehaen, *Chem. Commun.* **2006**, 266–268.

[6] M. Baruah, W. Qin, N. Basarić, W. M. De Borggraeve, N. Boens, *J. Org. Chem.* **2005**, *70*, 4152–4157.

[7] a) W. Qin, M. Baruah, M. Van der Auweraer, F. C. De Schryver, N. Boens, *J. Phys. Chem. A* **2005**, *109*, 7371–7384; b) W. Qin, T. Rohand, M. Baruah, A. Stefan, M. Van der Auweraer, W. Dehaen, N. Boens, *Chem. Phys. Lett.* **2006**, *420*, 562–568; c) W. Qin, T. Rohand, W. Dehaen, J. N. Clifford, K. Driesen, D. Beljonne, B. Van Averbeke, M. Van der Auweraer, N. Boens, *J. Phys. Chem. A* **2007**, *111*, 8588–8597; d) T. Rohand, J. Lycoops, S. Smout, E. Braeken, M. Sliwa, M. Van der Auweraer, W. Dehaen, W. M. De Borggraeve, N. Boens, *Photochem. Photobiol. Sci.* **2007**, *6*, 1061–1066; e) Z. Li, R. Bittman, *J. Org. Chem.* **2007**, *72*, 8376–8382; f) Z. Ekmekci, M. D. Yilmaz, E. U. Akkaya, *Org. Lett.* **2008**, *10*, 461–464; g) L. Li, J. Han, B. Nguyen, K. Burgess, *J. Org. Chem.* **2008**, *73*, 1963–1970; h) W. Qin, V. Leen, T. Rohand, W. Dehaen, P. Dedecker, M. Van der Auweraer, K. Robeyns, L.

Van Meervelt, D. Beljonne, B. Van Averbeke, J. N. Clifford, K. Driesen, K. Binnemans, N. Boens, *J. Phys. Chem. A* **2009**, *113*, 439–447; i) W. Qin, V. Leen, W. Dehaen, J. Cui, C. Xu, X. Tang, W. Liu, T. Rohand, D. Beljonne, B. Van Averbeke, J. N. Clifford, K. Driesen, K. Binnemans, M. Van der Auweraer, N. Boens, *J. Phys. Chem. C* **2009**, *113*, 11731–11740; j) K. Cieślik-Boczula, K. Burgess, L. Li, B. Nguyen, L. Pandey, W. M. De Borggraeve, M. Van der Auweraer, N. Boens, *Photochem. Photobiol. Sci.* **2009**, *8*, 1006–1015.

[8] a) C.-H. Lee, J. S. Lindsey, *Tetrahedron* **1994**, *50*, 11427–11440; b) G. Santosh, M. Ravikanth, *Tetrahedron* **2007**, *63*, 7833–7844.

[9] S. Rai, G. Gayatri, G. N. Sastry, M. Ravikanth, *Chem. Phys. Lett.* **2008**, *467*, 179–185.

[10] a) R. Ziessel, L. Bonardi, G. Ulrich, *Dalton Trans.* **2006**, 2913–2918; b) C. Bonnier, W. E. Piers, M. Parvez, T. S. Sorensen, *Chem. Commun.* **2008**, 4593–4595; c) T. W. Hudnall, F. P. Gabbaï, *Chem. Commun.* **2008**, 4596–4597; d) J. A. Jacobsen, J. R. Stork, D. Magde, S. M. Cohen, *Dalton Trans.* **2010**, *39*, 957–962.

[11] a) A. Costela, I. García-Moreno, C. Gomez, R. Sastre, F. Amat-Guerri, M. Liras, F. López Arbeloa, J. Bañuelos Prieto, I. López Arbeloa, *J. Phys. Chem. A* **2002**, *106*, 7736–7742; b) J. Bañuelos Prieto, F. López Arbeloa, V. Martínez Martínez, T. Arbeloa López, F. Amat-Guerri, M. Liras, I. López Arbeloa, *Chem. Phys. Lett.* **2004**, *385*, 29–35; c) F. López Arbeloa, J. Bañuelos Prieto, V. Martínez Martínez, T. Arbeloa Lopez, I. López Arbeloa, *ChemPhysChem* **2004**, *5*, 1762–1771.